arXiv:1201.2112v1 [cond-mat.quant-gas] 10 Jan 2012

Majorana Modes in Driven-Dissipative Atomic Superfluids With Zero Chern Number

C.-E. Bardyn,[1] M. A. Baranov,[2,3,4] E. Rico,[2,3] A. İmamoğlu,[1] P. Zoller,[2,3] and S. Diehl[2,3]

[1] *Institute for Quantum Electronics, ETH Zurich, 8093 Zurich, Switzerland*
[2] *Institute for Quantum Optics and Quantum Information of the Austrian Academy of Sciences, A-6020 Innsbruck, Austria*
[3] *Institute for Theoretical Physics, University of Innsbruck, A-6020 Innsbruck, Austria*
[4] *RRC "Kurchatov Institute", Kurchatov Square 1, 123182 Moscow, Russia*

We investigate dissipation-induced p-wave paired states of fermions in two dimensions and show that dissipation can break the bulk-edge correspondence present in Hamiltonian systems in a way that leads to the appearance of spatially separated Majorana zero modes in a phase with vanishing Chern number. We construct an explicit model of a dissipative vortex that traps a single of these modes and establish its topological origin by mapping it to a one-dimensional wire where we observe a non-equilibrium topological phase transition characterized by an abrupt change of a topological invariant (winding number). Engineered dissipation opens up possibilities for experimentally realizing such states with no Hamiltonian counterpart.

The search for topological phases of matter in which elementary excitations exhibit non-Abelian statistics have brought two-dimensional (2D) p-wave paired superfluids and superconductors –supporting isolated Majorana zero modes– to the forefront of theoretical and experimental condensed-matter research [1–5]. As a consequence of the bulk-edge correspondence found in the corresponding Hamiltonian systems [4, 6–8], *unpaired* Majorana fermions have been theoretically predicted to appear in vortices of odd vorticity and/or on edges if and only if the bulk of the system is characterized by an odd integer-valued topological invariant known as the Chern number.

In this Letter, we show that the widely accepted bulk-edge correspondence can be broken in 2D fermionic systems subject to dissipation, in such a way that isolated Majorana zero modes (MZMs) can be obtained in p-wave paired superfluid steady states with *even* Chern number. In contrast to recent discussions regarding the effects of decoherence on MZMs due to unwanted coupling to reservoirs [9, 10], we consider dissipation resulting from engineered reservoirs.

The starting point of our analysis is the construction of a purely dissipative dynamics governed by a Lindblad master equation [11] that drives spinless fermions on a square lattice into a complex p-wave paired state with Chern number $\nu_{2\mathrm{D}} = 0$. We investigate the system in a geometry corresponding to a (dissipative) vortex of vorticity $l = 1$, and show that it maps to a 1D chiral fermion problem [12] characterized by a non-trivial topological invariant (winding number) $\nu_{1\mathrm{D}} = 2$. Although this suggests the existence of two MZMs in the vortex core, we demonstrate that the core only supports a *single* of these modes, in contradiction with the bulk-edge correspondence. We relate this striking observation to our dissipative boundary conditions –imposed by the vortex geometry alone– and thereby establish a mechanism that ultimately allows us to create (dissipative) non-Abelian vortices despite the vanishing Chern number of the bulk. This effect crucially relies on dissipation and has no Hamiltonian counterpart.

We show that our results hold over an extended parameter range which defines a topologically non-trivial phase, and establish for the first time a non-equilibrium topological phase transition signaled by divergent length and time scales [13–16] and a discontinuity in the winding number. Finally, we propose a scheme to generate the MZMs dynamically in a driven-dissipative system of atomic fermions through optical vortex imprinting [17].

Dissipative framework – We consider a system of N fermionic sites $a_i^\dagger, a_i$ evolving under a purely dissipative dynamics governed by a Lindblad master equation

$$\partial_t \rho = \kappa \sum_{i=1}^{N} \left(L_i \rho L_i^\dagger - \tfrac{1}{2}\{L_i^\dagger L_i, \rho\} \right), \qquad (1)$$

where ρ is the system density matrix, κ the damping rate, and L_i are Lindblad operators which are linear in the fermionic operators. The steady state of such dynamics is pure –and therefore can be viewed as a ground state of the effective Hamiltonian $H_{\mathrm{eff}} \equiv \sum_i L_i^\dagger L_i$– if and only if the Lindblad operators form a set of anticommuting operators, i.e. $\{L_i, L_j\} = 0 \ \forall i, j = 1, \ldots, N$, although purity is not required for the existence of topological order [11]. The counterpart of topological ground-state degeneracy is the existence of a nonlocal decoherence-free subspace protected by a dissipative gap and associated

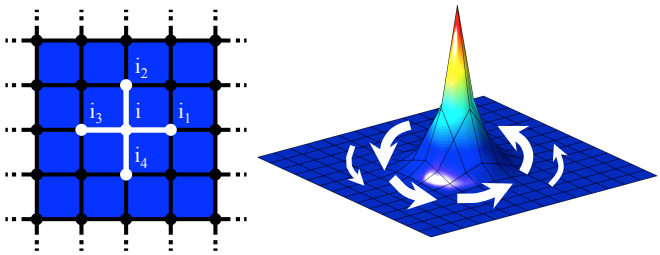

FIG. 1. (color online). Graphical representation of the cross Lindblad operator in Eq. (2) (left) and typical form of a MZM trapped in a dissipative $l = 1$ vortex (right).

with zero-damping Majorana modes $\gamma = \gamma^\dagger$ satisfying the orthogonality condition $\{L_i, \gamma\} = 0\ \forall i$.

The differences between Hamiltonian and dissipative dynamics that are crucial to this work can be discussed concisely in a matrix representation of (1) obtained by introducing a basis of Majorana operators $c_{2i-1} = a_i^\dagger + a_i$, $c_{2i} = \mathrm{i}(a_i^\dagger - a_i)$ [15, 18]. Using the fact that (1) is quadratic and assuming Gaussian initial states, one can focus exclusively on the time evolution of the correlation matrix $\Gamma_{ij} = (\mathrm{i}/2)\,\mathrm{tr}([c_i, c_j]\rho)$. The purity of the state is then reflected in the spectrum of Γ^2; in particular, a mode $\tilde{\gamma} = \mathbf{v}^T\mathbf{c}$ (where $\mathbf{c}^T = (c_1, c_2, \ldots, c_{2N})$) corresponding to an eigenvector $\mathbf{v}$ of Γ^2 with eigenvalue zero is associated with a completely mixed subspace and will be referred to as a purity zero mode [19]. Writing the Lindblad operators as $L_i = \mathbf{l}_i^T\mathbf{c}$, one finds the equation of motion $\partial_t\Gamma = -\{X, \Gamma\} + Y$ for $\kappa = 1$, where $X = 2\,\mathrm{Re}\,M$ and $Y = 4\,\mathrm{Im}\,M$ with $M = \sum_i \mathbf{l}_i \otimes \mathbf{l}_i^\dagger$. Physically, the real symmetric matrix X describes the damping. Its eigenvectors $\mathbf{w}_i$ are associated with Majorana modes $\bar{\gamma}_i = \mathbf{w}_i^T\mathbf{c}$ $(= \bar{\gamma}_i^\dagger)$ which decay exponentially with damping rates $\kappa_i \geq 0$ given by the corresponding eigenvalues; if $\kappa_i = 0$, $\bar{\gamma}_i$ is a MZM. The real antisymmetric matrix Y, on the other hand, determines the fluctuations in the steady state $\tilde{\Gamma}$ through the relation $\{X, \tilde{\Gamma}\} = Y$ and is the counterpart of the effective Hamiltonian in the matrix representation since $H_{\text{eff}} = \frac{\mathrm{i}}{4}\mathbf{c}^T Y \mathbf{c}$.

The damping matrix X solely determines the existence of zero modes. Crucially, a zero mode of H_{eff} (or $\mathrm{i}Y$) does not necessarily correspond to a zero mode of X, whereas the converse is always true (see [20]). Any zero mode of H_{eff} which does not coincide with a zero mode of X is effectively traced out of the system in steady state and emerges as an *intrinsic* purity zero mode, *independent* of the initial conditions. As shown below, this opens the door to interesting dissipative effects such as the breakdown of the bulk-edge correspondence pertaining to Hamiltonian systems [4, 6–8].

These deviations resulting from dissipation are crucially rooted in the fact that the well-known Hamiltonian mechanisms of topological protection embedded in H_{eff} do not extend to X. Indeed, while the antisymmetry of Y alone ensures that the MZMs of H_{eff} come in pairs and therefore are not affected by local perturbations when spatially separated (see [20] for further details), the symmetry of X does not provide for such a mechanism and MZMs are generally not protected against arbitrary local dissipative perturbations. Below we show that the potentially harmful effects of dissipation (discussed in another context in [9, 10]) can also lead to intriguing physical effects such as the transformation of Abelian vortices into non-Abelian ones.

The model – We consider a square-lattice system driven by *cross* Lindblad operators defined as the following quasi-local linear superposition of fermionic creation and annihilation operators $a_i^\dagger, a_i$:

$$L_i = C_i^\dagger + s\,e^{\mathrm{i}\varphi}A_i = \beta\,a_i^\dagger + (a_{i_1}^\dagger + a_{i_2}^\dagger + a_{i_3}^\dagger + a_{i_4}^\dagger) + s\,e^{\mathrm{i}\varphi}(a_{i_1} + \mathrm{i}a_{i_2} - a_{i_3} - \mathrm{i}a_{i_4}), \tag{2}$$

where $\beta \in \mathbb{R}$, $s > 0$ and i_1, i_2, i_3 and i_4 are the four nearest-neighboring sites of i, as illustrated in Fig. 1. The dissipative dynamics (1) generated by such Lindblad operators can be obtained, for example, in the long-time evolution of a microscopically number-conserving (quartic) dissipative dynamics generating phase-locked paired states [11, 21]. In that context, the global relative phase φ between creation and annihilation parts emerges through spontaneous symmetry breaking of the global $U(1)$ symmetry, and the relative strength s is determined by the average particle number. The dimensionless parameter β, on the other hand, can be used to tune the system across quantum phase transitions.

The bulk properties of the system can be revealed in an infinite system with periodic boundary conditions, in which case the problem is readily solved in momentum space. Defining coefficients u_{ij}, v_{ij} such that $L_i = \sum_j (u_{ij}a_j + v_{ij}a_j^\dagger)$, the momentum-space cross Lindblad operators take the form $L_{\mathbf{k}} = u_{\mathbf{k}}a_{\mathbf{k}} + v_{\mathbf{k}}a_{-\mathbf{k}}^\dagger$, where $u_{\mathbf{k}}, v_{\mathbf{k}}$ are the Fourier transforms of u_{ij}, v_{ij}. Properly normalized, they become Bogoliubov-Valatin quasiparticle operators associated with damping rates $\kappa_{\mathbf{k}} = \kappa\mathcal{N}_{\mathbf{k}}$, where $\mathcal{N}_{\mathbf{k}} = \xi_{\mathbf{k}}^\dagger\xi_{\mathbf{k}}$ with $\xi_{\mathbf{k}}^T = (u_{\mathbf{k}}, v_{\mathbf{k}})$. Since the cross Lindblad operators form a complete set of anticommuting operators, the system is driven into a unique and pure complex p-wave paired state $|\Omega\rangle$ defined by the condition $L_{\mathbf{k}}|\Omega\rangle = 0$ for all $\mathbf{k}$ and fully characterized by the real vector $\mathbf{n}_{\mathbf{k}} = \xi_{\mathbf{k}}^\dagger\boldsymbol{\sigma}\xi_{\mathbf{k}}$, where $\boldsymbol{\sigma}$ is a vector of Pauli matrices. Such a state can be characterized by a topological invariant $\nu_{2\text{D}}$ known as the Chern number; we find here

$$\nu_{2\text{D}} \equiv \tfrac{1}{4\pi}\int_{\text{BZ}} d^2\mathbf{k}\ \mathbf{n}_{\mathbf{k}} \cdot (\partial_{k_x}\mathbf{n}_{\mathbf{k}} \times \partial_{k_y}\mathbf{n}_{\mathbf{k}}) = 0 \tag{3}$$

(where BZ stands for Brillouin zone) for all values of β except at the isolated critical points $\beta_c = 0, \pm 4$ where the dissipative gap closes, leading to divergent length and time scales [15, 16] characteristic of a second-order phase transition, while preserving the symmetry of the state encoded in $\mathbf{n}_{\mathbf{k}}$. Since there is no extended parameter range with non-trivial topological order, one naively expects topological features such as isolated MZMs to be absent when edges or vortices are introduced.

Existence of isolated MZMs – We now demonstrate in three main steps that the above dissipative system can support spatially separated MZMs despite its seemingly trivial topological nature. We first study the system in cylinder geometry and show the existence of two isolated MZMs for $0 < |\beta| < 4$ under specific dissipative boundary conditions. Next, we establish the topological origin of

these modes by mapping the system to a 1D model and identifying a non-trivial topological invariant (cf. [22, 23] for conceptually similar approaches). Finally, we show that the cylinder model is equivalent to a planar model with a single MZM trapped into a dissipative vortex of vorticity $l = 1$.

i) Square-lattice model in cylinder geometry – We consider a system of $N = N_x \times N_y$ sites in a cylinder geometry defined by imposing open boundary conditions in the x-direction and periodic boundary conditions in the y-direction, and associate *truncated* cross Lindblad operators $\bar{L}_{i,L}(\bar{L}_{i,R})$ with the sites i of the left (right) edges of the cylinder –which we define by setting the left (right) arm of (2) to zero. With this choice of dissipative boundary conditions, we find exactly *two* isolated MZMs in the parameter range $0 < |\beta| < 4$ (see [20] for their explicit construction), which we denote as γ_L (γ_R) in accordance with their localization on the left (right) edges of the cylinder. While uniformly spread along the y-direction, these modes appear as exponentially localized in the x-direction, on a characteristic length scale $\xi = \xi(|\beta|) \sim 1/|\log|1 - |\beta|/2||$ which diverges at $\beta_c = 0, \pm 4$. At these critical values of β, the norm of $\gamma_{L,R}$ diverges with N_y and the dissipative gap closes in the bulk, which indicates the onset of a non-equilibrium topological quantum phase transition. Since $|\{\bar{L}_{i,R}, \gamma_L\}| = |\{\bar{L}_{i,L}, \gamma_R\}| \sim (1 - |\beta|/2)^{N_x}$, $\gamma_{L,R}$ correspond to small damping rates $\lambda_{L,R} \sim N_y(1 - |\beta|/2)^{2N_x}$ which decrease exponentially with the system size N_x, i.e. with the distance between γ_L and γ_R (see [20]). The situation is thus reminiscent of that of interacting Majorana modes in a Hamiltonian system: $|\beta| \neq 2$ can be viewed as a coupling constant and $\lambda_{L,R}$ as small splittings of the Majorana modes caused by inter-edge tunneling.

The appearance of two MZMs can be traced back to the existence of two gapless edge modes in the damping spectrum in the limit $N_y \to \infty$, as verified numerically. Crucially, a single gapless mode is found on each of the edges, although the well-known bulk-edge correspondence for the Chern number [4, 6–8] would suggest the existence of an even number of them. This apparent contradiction can be resolved by remembering that the bulk-edge correspondence only applies to the effective Hamiltonian $H_{\text{eff}} = \sum_i L_i^\dagger L_i$ (or to the matrix iY); not to the damping matrix X. Since the Lindblad operators anticommute with each other in the bulk, the bulk spectrum and eigenmodes of H_{eff} exactly coincide with those of X. However, since our dissipative boundary conditions do not satisfy such anticommutation relations, the situation changes drastically on the edges. In light of the general discussion above, we expect the absence of bulk-edge correspondence to be intimately related to the closing of the "gap" associated with the purity spectrum.

ii) Mapping to a 1D model: topological origin of the MZMs – The discrete rotational symmetry of the cylinder translates to a discrete translational symmetry along the y-direction and implies that momentum is conserved in that direction. As a result, the dissipative dynamics splits into decoupled momentum sectors described by the Fourier-transformed Lindblad operators $L_x(k_y) \propto \sum_y e^{-ik_y y} L_{x,y}$ (where (x, y) are position-space coordinates), and the system effectively reduces to a stack of 1D systems which can be characterized by an integer topological invariant (winding number) ν_{1D} thanks to their chiral symmetry [11, 24]. Since the MZMs $\gamma_{L,R}$ can only be constructed when $N_y \geq 1$ if $\beta < 0$ and when N_y is even if $\beta > 0$ (see [20]), they must belong to the sector $k_y = 0$ when $\beta < 0$ and $k_y = \pi$ when $\beta > 0$. In both sectors, the momentum space cross Lindblad operators take the form

$$L_i = \beta' \, a_i^\dagger + (a_{i-1}^\dagger + a_{i+1}^\dagger) + (-a_{i-1} + a_{i+1}), \quad (4)$$

where $L_i \equiv L_x(k_y = 0, \pi)$ and $\beta' = \beta + 2$ ($\beta - 2$) if $\beta < 0$ (> 0). We then obtain

$$\nu_{1D} \equiv \tfrac{1}{2\pi} \int_{BZ} dk \; \mathbf{a} \cdot (\mathbf{n}_k \times \partial_k \mathbf{n}_k) = 2 \quad (5)$$

for $|\beta'| < 2$ (i.e. for $0 < |\beta| < 4$) and $\nu_{1D} = 0$ otherwise ($\mathbf{a}$ being a unit vector orthogonal to $\mathbf{n}_k$ for all k whose existence is guaranteed by chiral symmetry). Therefore, the parameter range $0 < |\beta| < 4$ in which the MZMs $\gamma_{L,R}$ are found exactly coincides with the one in which the system exhibits non-trivial topological order. A non-equilibrium topological quantum phase transition occurs at the critical values $\beta_c = \pm 4$, while $\beta_c = 0$ appears as an isolated critical point separating two topologically equivalent phases. In agreement with the results obtained above for the full 2D problem, the damping gap closes at each of these values.

In accordance with the bulk-edge correspondence, (5) shows the existence of $\nu_{1D} = 2$ gapless chiral edge modes of H_{eff} on each of the edges of the cylinder, with an associated pair of MZMs that is topologically protected as long as the chiral symmetry of the system is preserved. Due to our dissipative boundary conditions, only one of these modes (on each edge) coincides with a MZM of X; the other acquires a non-zero damping rate and is effectively traced out of the system, thereby emerging as an intrinsic purity zero mode.

iii) Construction of dissipative vortices – Next, we show that dissipative $l = 1$ vortices trapping single MZMs naturally arise from spatial deformations of our cylinder model. For notational simplicity, we work in the continuum limit, in which the cross Lindblad operators take the form $L(x, y) = ((\beta + 4) + \partial_x^2 + \partial_y^2)\, \psi^\dagger(x, y) + (\partial_x + i\partial_y)\, \psi(x, y)$ where $\psi(x, y)$ denotes the fermionic field and (x, y) are local Cartesian coordinates on the surface S in which the system is embedded. Since the (extrinsic) curvature of S is seen by the cross Lindblad operators as a gauge field [1], the only way to continuously deform the system while preserving its properties

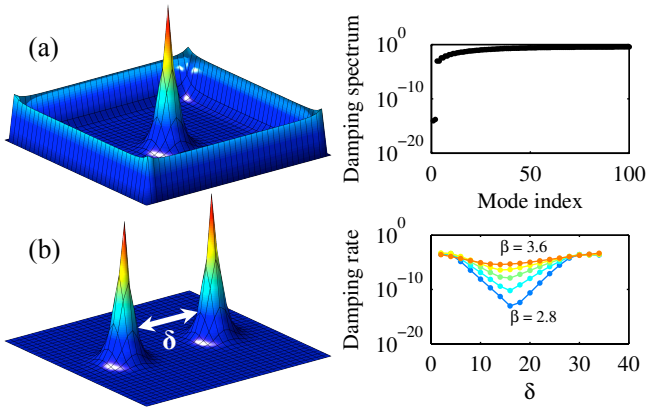

FIG. 2. (color online). Numerical results for a square lattice of 35×35 sites with unit spacing and $\kappa = 1$. (a) One-vortex configuration: typical form of the MZMs (here for $\beta = 3$) localized in the vortex core and on the edge, respectively (left), and low-lying part of the damping spectrum for $\beta = 2$, featuring a gap with two zero eigenvalues (right). (b) Two-vortex configuration: typical form of the MZMs localized in each of the vortex cores, respectively (left), and behavior of their residual damping rate as a function of the vortex separation δ, for different values of β (right). All results were obtained for vanishingly small vortex cores.

(such as the existence of MZMs) is to introduce an *external* $U(1)$ gauge field. This mechanism can be illustrated by considering a simple mapping from S to an annulus with $x \mapsto r$, $y \mapsto r\varphi$, where r, φ are polar coordinates on the annulus with origin at its center: one finds $(\partial_x + \mathrm{i}\partial_y) \mapsto (\partial_r + \mathrm{i}\partial_\varphi/r) = e^{-\mathrm{i}\varphi}(\partial_{x'} + \mathrm{i}\partial_{y'})$ where x', y' are Cartesian coordinates on the annulus, and the deformed cross Lindblad operators become $L(x', y') = ((\beta + 4) + \partial^2_{x'} + \partial^2_{y'})\,\psi^\dagger(x', y') + e^{-i\varphi}(\partial_{x'} + \mathrm{i}\partial_{y'})\,\psi(x', y')$ and thus acquire a phase φ that cannot be eliminated by a gauge transformation. The continuous deformation of S into (a) a finite plane with one hole or (b) a sphere with two holes generally results in a single half-flux quantum of the gauge field attached to each hole, thus giving rise to one-vortex or two-vortex configurations, respectively. Based on these considerations, we define a dissipative vortex as (i) a hole in the lattice (with dissipative boundary conditions in the form of truncated Lindblad operators connecting to a topologically trivial vacuum state in the core) and (ii) a site-dependent phase factor $\varphi_i = l\,\varphi(\mathbf{r}_i)$ multiplying the annihilation part of the Lindblad operators (2), where $l = 1$ is the vorticity, $\mathbf{r}_i$ the position vector of the site i as measured from the center of the hole, and $\varphi(\mathbf{r}_i) \in [0, 2\pi)$ the associated phase in polar coordinates.

The one-to-one correspondence between the analytically tractable cylinder model and configurations of dissipative $l = 1$ vortices on the plane has been verified through numerical calculations, both for one- and two-vortex configurations (cf. Fig. 2). Our numerical studies confirm the existence of MZMs for $0 < |\beta| < 4$. In both one- and two-vortex configurations, the damping spectrum features two zero modes (cf. (a)) and the purity spectrum (not shown) exhibits a similar form with two intrinsic purity zero modes signaling the purely dissipative nature of our model. As shown in (b), the exponential decay of the residual damping rate of the MZMs with the vortex separation was also verified in a two-vortex configuration.

Implementation in ultracold atom systems – The ingredients of a dissipative vortex are (i) its phase and (ii) a core with dissipative boundary conditions that crucially affect the purity of the state. As verified numerically, such a situation naturally arises in a microscopically number-conserving implementation where the quasi-local creation ($C_i^\dagger$) and annihilation (A_i) parts of the bilinear Lindblad operators $L_i = C_i^\dagger A_i$ result from different physical processes [11, 21, 25]. The annihilation part can be obtained through coherent driving, i.e. $A_i = \sum_j \Omega_{ij} a_j$, where Ω_{ij} is the Rabi frequency connecting to an auxiliary degree of freedom such as the intermediate site of an optical superlattice. In particular, the short-distance p-wave structure can be realized with specific wavelength ratios and relative phases of lattice and driving lasers, while the longer-range vortex profile can be implemented with a drive laser carrying an optical vortex (as obtained e.g. in the far-field regime of a fork hologram or a spiral phase plate [26]); this results in Rabi frequencies of the form $\Omega_{ij} \sim g(r_j, \varphi_j)[\delta_{i-\mathbf{e}_x,j} - \delta_{i+\mathbf{e}_x,j} + \mathrm{i}(\delta_{i-\mathbf{e}_y,j} - \delta_{i+\mathbf{e}_y,j})]$, where g is a slowly varying function proportional to the laser amplitude encoding the optical vortex, e.g. $g(r, \varphi) \sim (r/l)e^{-(r/\xi)^2}e^{\mathrm{i}\varphi}$ with $l, \xi \gg a$ (a being the lattice spacing). In contrast, the creation part results from spontaneous emission from the auxiliary site and is generically isotropic, thus giving $C_i^\dagger$ the desired s-wave symmetry. As mentioned before, the Lindblad operators (2) then arise in the long-time thermodynamic limit, in which a dissipative mean-field theory based on the proximity to the known stationary state can be constructed [11, 21].

Conclusions – We have shown that 2D lattice fermions can be dissipatively driven into a phase supporting spatially separated MZMs despite a trivial bulk Chern number. This extends the concept of topological order in driven-dissipative ensembles [11] to 2D systems –possibly with enhanced practicality, since dissipative vortices can directly be obtained by imprinting the quantized angular momentum of light onto the matter system [17]. Most importantly, it shows that dissipation does not necessarily act destructively on the Majorana edge physics, but can lead to intriguing novel effects.

The authors would like to thank S. Habraken, V. Gurarie, V. Lahtinen and J. Pachos for insightful discussions. This work was supported by NCCR Quantum Science and Technology (NCCR QSIT), research instrument of the Swiss National Science Foundation (SNSF),

an ERC Advanced Investigator Grant (A.I.), the Austrian Science Fund (FWF) through SFB FOQUS and the START grant Y 581-N16 (S. D.), the European Commission (AQUTE, NAMEQUAM), the Institut fuer Quanteninformation GmbH and the DARPA OLE program.

[1] N. Read, D. Green, Phys. Rev. B**61**, 10267-10297 (2000).
[2] D. A. Ivanov, Phys. Rev. Lett. **86**, 268-271 (2001).
[3] A. Yu. Kitaev, Ann. Phys. **303** 2–30 (2003).
[4] A. Yu. Kitaev, Ann. Phys. **321** 2 (2006).
[5] C. Nayak, S. H. Simon, A. Stern, M. Freedman, and S. Das Sarma, Rev. Mod. Phys. **80**, 1083 (2008).
[6] Y. Hatsugai, Phys. Rev. Lett. **71** 3697 (1993).
[7] S. Ryu, A. Schnyder, A. Furusaki, A. W. W. Ludwig, New J. Phys. **12**, 065010 (2010).
[8] V. Gurarie, Phys. Rev. B **83** 085426 (2011); A. M. Essin and V. Gurarie, Phys. Rev. B **84**, 125132 (2011).
[9] G. Goldstein, C. Chamon, Phys. Rev. B **85**, 205109 (2011).
[10] J. C. Budich, S. Walter, B. Trauzettel, arXiv:1111.1734 (2011).
[11] S. Diehl, E. Rico, M. A. Baranov, P. Zoller, Nat. Phys. **7**, 971 (2011).
[12] A. Yu. Kitaev, Physics-Uspekhi **44**, 131 (2001).
[13] F. Verstraete, M. M. Wolf, and J. I. Cirac, Nature Phys. **5**, 633 (2009).
[14] S. Diehl *et al.*, Phys. Rev. Lett. **105**, 015702 (2010); A. Tomadin *et al.*, Phys. Rev. A **83**, 013611 (2011).
[15] J. Eisert and T. Prosen, arXiv:1012.5013 (2010).
[16] M. Hoening, M. Moos, M. Fleischhauer, arXiv:1108.2263 (2011).
[17] J. F. S. Brachmann *et al.*, arXiv:1102.3373 (2011).
[18] T. Prosen, New J. Phys. 10, 043026 (2008); T. Prosen, J. Stat. Mech. P07020 (2010).
[19] Due to the antisymmetry of Γ, such modes must always come in pairs.
[20] See online supplementary material.
[21] S. Diehl, W. Yi, A. J. Daley, P. Zoller, Phys. Rev. Lett. **105**, 227001 (2010); W. Yi, S. Diehl, A. J. Daley, P. Zoller, arXiv:1111.7053 (2011).
[22] S. Tewari, S. Das Sarma, D.-H. Lee, Phys. Rev. Lett. **99**, 037001 (2007).
[23] C.-Y. Hou, C. Chamon, C. Mudry, Phys. Rev. Lett. **98** 186809 (2007).
[24] S. Ryu, Y. Hatsugai, Phys. Rev. Lett. **89**, 077002 (2002).
[25] S. Diehl *et al.*, Nature Phys. **4**, 878 (2008).
[26] N. R. Heckenberg, R. McDuff, C. P. Smith, A. G. White, Optics Letters **17** , 221 (1992); L. Allen, M. W. Beijersbergen, R. J. C. Spreeuw, J. P. Woerdman, Phys. Rev. A **45**, 8185 (1992); G. Molina-Terriza, J. P. Torres, L. Torner, Nat. Phys. **3**, 305 (2007).

Supplementary Material for "Majorana Modes in Driven-Dissipative Atomic Superfluids With Zero Chern Number"

C.-E. Bardyn,[1] M. A. Baranov,[2,3,4] E. Rico,[2,3] A. İmamoğlu,[1] P. Zoller,[2,3] and S. Diehl[2,3]

[1] *Institute for Quantum Electronics, ETH Zurich, 8093 Zurich, Switzerland*
[2] *Institute for Quantum Optics and Quantum Information of the Austrian Academy of Sciences, A-6020 Innsbruck, Austria*
[3] *Institute for Theoretical Physics, University of Innsbruck, A-6020 Innsbruck, Austria*
[4] *RRC "Kurchatov Institute", Kurchatov Square 1, 123182 Moscow, Russia*

arXiv:1201.2112v1 [cond-mat.quant-gas] 10 Jan 2012

Majorana zero modes and decoherence-free subspaces – The $2N \times 2N$ real symmetric damping matrix X and real antisymmetric fluctuation matrix Y encoding the dissipative dynamics are defined in the main text. By construction, X is positive semidefinite and can be spectrally decomposed as $X = \sum_{j=1}^{2N} \lambda_j (\mathbf{v}_j^T \otimes \mathbf{v}_j)$ with eigenvalues $\lambda_j \in \mathbb{R}_{\geq 0}$ and associated eigenvectors $\mathbf{v}_j \in \mathbb{R}^{2N}$. The vectors $\mathbf{v}_j$ are real and form an orthonormal basis; they define a natural Majorana basis $\gamma_j \equiv \mathbf{v}_j^T \mathbf{c}$ ($j = 1, 2, \ldots, 2N$) associated with X. The fact that they are real also implies that $\mathbf{l}_i^\dagger \mathbf{v}_j = (\mathbf{l}_i^T \mathbf{v}_j)^*$ for all j, so that $X_{jk} \equiv \mathbf{v}_j^T X \mathbf{v}_k = 2 \sum_{i=1}^N \mathrm{Re}\,\{(\mathbf{l}_i^T \mathbf{v}_j)(\mathbf{l}_i^T \mathbf{v}_k)^*\} = \lambda_j \, \delta_{ij}$ with $\lambda_j = 2 \sum_{i=1}^N |\mathbf{l}_i^T \mathbf{v}_j|^2$, and $Y_{jk} \equiv \mathbf{v}_j^T Y \mathbf{v}_k = 4 \sum_{i=1}^N \mathrm{Im}\,\{(\mathbf{l}_i^T \mathbf{v}_j)(\mathbf{l}_i^T \mathbf{v}_k)^*\}$. The eigenvalues λ_j physically correspond to the damping rates associated with the Majorana modes γ_j and are solely determined by the amount of overlap $\mathbf{l}_i^T \mathbf{v}_j$ between the eigenvectors $\mathbf{v}_j$ and the vectors $\mathbf{l}_i$ associated with the Lindblad operators L_i in the original (local) Majorana basis. Since $\mathbf{l}_i^T \mathbf{v}_j = \{L_i, \gamma_j\}$, the damping rates can alternatively be seen as determined by the amount by which the Majorana modes γ_j anticommute with the Lindblad operators L_i. In general, we refer to a Majorana mode γ_j as a Majorana *zero* mode if and only if the associated damping rate λ_j vanishes. In light of the above considerations, we thus conclude that a normalized vector $\mathbf{v} \in \mathbb{R}^{2N}$ defines a Majorana zero mode $\gamma = \mathbf{v}^T \mathbf{c}$ if and only if the following equivalent conditions are satisfied:

(i) $X\mathbf{v} = 0$.

(ii) $\mathbf{l}_i^T \mathbf{v} = 0$ for all $i \in \{1, 2, \ldots, n\}$.

(iii) $\{L_i, \gamma\} = 0$ for all $i \in \{1, 2, \ldots, n\}$.

Remembering the explicit form of the matrix Y, these conditions also imply $Y\mathbf{v} = 0$ (the converse, however, is generally not true). As a result, $\mathbf{v}$ must be a simultaneous eigenvector of both the damping and the fluctuation matrices with zero eigenvalue. We note that the dimension of the decoherence-free subspace associated with $m \leq 2N$ Majorana zero modes is $2^{(m - m \bmod 2)}$. This stems from the fact that the state space of the (Gaussian) system is isomorphic to the space of all real $2N \times 2N$ antisymmetric correlation matrices Γ (see the main text for the associated equation of motion). As a consequence, the kernel of this matrix –which is decoupled from the dissipative dynamics– must have even dimension and m Majorana zero modes generally lead to a $(m - m \bmod 2)$-dimensional space which is unaffected by dissipation. In conclusion, only *pairs* of Majorana zero modes can be decoupled from dissipation.

Robustness of the Majorana zero modes – We consider the case where the dissipative dynamics generated by n Lindblad operators L_i gives rise to $m \leq 2N$ Majorana zero modes $\gamma_\alpha = \mathbf{v}_\alpha^T \mathbf{c}$. We define V_0 as the m-dimensional subspace associated with these modes and use Greek indices to denote quantities pertaining to the latter. We also assume that there exist Gaussian initial correlations between the Majorana zero modes, which we collect in an initial covariance matrix $\Gamma_{\alpha\beta}(t = 0) \equiv (\mathrm{i}/2)\,\mathrm{tr}([\gamma_\alpha, \gamma_\beta]\rho(t = 0))$. By definition, the dissipative dynamics restricted to the subspace V_0 is trivial, namely, $\partial_t \Gamma_{\alpha\beta} = 0$. In order to examine under what conditions it remains trivial, we extend the dissipative dynamics by introducing an additional Lindblad operator $L_{n+1} = \mathbf{l}_{n+1}^T \mathbf{c}$. In that case, the X and Y matrices (which were identically zero in V_0) become

$$X_{\alpha\beta} \equiv \mathbf{v}_\alpha^T X \mathbf{v}_\beta = 2\ \mathrm{Re}\,\{(\mathbf{l}_{n+1}^T \mathbf{v}_\alpha)(\mathbf{l}_{n+1}^T \mathbf{v}_\beta)^*\} \tag{1}$$

$$Y_{\alpha\beta} \equiv \mathbf{v}_\alpha^T Y \mathbf{v}_\beta = 4\ \mathrm{Im}\,\{(\mathbf{l}_{n+1}^T \mathbf{v}_\alpha)(\mathbf{l}_{n+1}^T \mathbf{v}_\beta)^*\} \tag{2}$$

Assuming that L_{n+1} acts quasi-locally and that the Majorana zero modes are localized and spaced sufficiently far away from each other –such that $\{\gamma_\alpha, \gamma_\beta\} = v_\alpha^T v_\beta = 0$ up to exponentially small corrections, two cases can occur: (i) either $\mathbf{l}_{n+1}^T \mathbf{v}_\alpha = \{L_{n+1}, \gamma_\alpha\} = 0$ for all $\alpha \in \{1, 2, \ldots, m\}$, or (ii) $\mathbf{l}_{n+1}^T \mathbf{v}_\mu = \{L_{n+1}, \gamma_\mu\} \neq 0$ for a single $\mu \in \{1, 2, \ldots, m\}$. Clearly, the dissipative dynamics remains unchanged in the first case. In particular, the Majorana zero modes survive and all initial correlations in V_0 are preserved over arbitrary long times. In the second case, however, the situation changes: although the off-diagonal elements of X and Y remain zero due to the local nature of L_{n+1} and of the γ_α (so that Y remains identically zero due to its antisymmetry), some of the diagonal entries of the symmetric matrix X become non-zero. More specifically, the Majorana mode γ_μ acquires a non-trivial damping rate $\lambda_\mu = |\mathbf{l}_{n+1}^T \mathbf{v}_\mu|^2 \neq 0$ (independent of the system size) due to the local dissipative perturbation corresponding to L_{n+1}, and the dissipative dynamics becomes $\partial_t \Gamma_{\alpha\mu} = -\lambda_\mu \Gamma_{\alpha\mu}$ for all $\alpha \in \{1, 2, \ldots, m\}$. We thus find that the introduction of an additional quasi-local Lindblad operator L_{n+1} which anticommutes with all Majorana zero modes but γ_μ has the effect of removing all non-local correlations involving the latter. After a time $t \sim 1/\lambda_\mu$, γ_μ is effectively traced out of the system, which generally results in a loss of purity (assuming that there was initial non-local correlations between γ_μ and the other Majorana zero modes).

Majorana zero modes in a square-lattice model wrapped on a cylinder – We consider a two-dimensional system of spinless fermions $a_i^\dagger, a_i$ on a square lattice of $N = N_x \times N_y$ sites, in a cylinder geometry defined by imposing open boundary conditions in the x-direction and periodic boundary conditions in the y-direction. We number the sites from left to right and top to bottom with indices $i \in \{1, 2, \ldots, N\}$ and distinguish three disjoint subsets of indices $\mathcal{L}$, $\mathcal{R}$ and $\mathcal{B}$ containing the sites i belonging respectively to the left and right edges of the cylinder, and to the bulk. We then associate to each site $i \in \mathcal{B}$ a cross Lindblad operator L_i as defined in Eq. (2) in the main text (with $s = 1$ and $\varphi = 0$, for simplicity). The corresponding vector $\mathbf{l}_i \in \mathbb{C}^{2N}$, defined such that $L_i = \mathbf{l}_i^T \mathbf{c}$, takes the explicit form

$$\begin{aligned}
\mathbf{l}_i^T = (\ \ldots\ ;\ 0,0\ ;\ \underbrace{e^{i\pi/4}/\sqrt{2}, -e^{i\pi/4}/\sqrt{2}}_{i-N_x}\ ;\ 0,0\ ;\ \ldots \\
\ldots\ ;\ \underbrace{0,-i}_{i-1}\ ;\ \underbrace{\beta/2, -i\beta/2}_{i}\ ;\ \underbrace{1,0}_{i+1}\ ;\ \ldots \\
\ldots\ ;\ 0,0\ ;\ \underbrace{e^{-i\pi/4}/\sqrt{2}, e^{-i\pi/4}/\sqrt{2}}_{i+N_x}\ ;\ 0,0\ ;\ \ldots\ )
\end{aligned} \tag{3}$$

where, in the above notation, the pairs of components $(\mathbf{l}_i)_{2j-1}$ and $(\mathbf{l}_i)_{2j}$ corresponding to the same site $j \in \{1, 2, \ldots, N\}$ are separated by semicolons and organized in the same two-dimensional way as the sites j on the lattice. For the sake of clarity, all non-zero pairs of components are indicated by braces and the index j of the site to which they correspond is shown explicitly. For $\beta < 0$, the two following vectors $\mathbf{v}_L, \mathbf{v}_R \in \mathbb{R}^{2N}$ are orthogonal to all $\mathbf{l}_i$ with $i \in \mathcal{B}$:

$$\begin{aligned}
\mathbf{v}_L^T = \Big(\ & +(\ 0,0\ ;\ 1,0\ ;\ (1-|\beta|/2),0\ ;\ (1-|\beta|/2)^2,0\ ;\ \ldots\ ;\ (1-|\beta|/2)^{N_x-2},0\ ;) \\
& -(\ 0,0\ ;\ 1,0\ ;\ (1-|\beta|/2),0\ ;\ (1-|\beta|/2)^2,0\ ;\ \ldots\ ;\ (1-|\beta|/2)^{N_x-2},0\ ;) \\
& +(\ 0,0\ ;\ 1,0\ ;\ (1-|\beta|/2),0\ ;\ (1-|\beta|/2)^2,0\ ;\ \ldots\ ;\ (1-|\beta|/2)^{N_x-2},0\ ;) \\
& \quad \ldots \\
& -(\ 0,0\ ;\ 1,0\ ;\ (1-|\beta|/2),0\ ;\ (1-|\beta|/2)^2,0\ ;\ \ldots\ ;\ (1-|\beta|/2)^{N_x-2},0\ )\ \Big)
\end{aligned} \tag{4}$$

$$\begin{aligned}
\mathbf{v}_R^T = \Big(\ & +(\ 0,(1-|\beta|/2)^{N_x-2}\ ;\ 0,(1-|\beta|/2)^{N_x-3}\ ;\ \cdots\ ;\ 0,1\ ;\ 0,0\ ;) \\
& -(\ 0,(1-|\beta|/2)^{N_x-2}\ ;\ 0,(1-|\beta|/2)^{N_x-3}\ ;\ \cdots\ ;\ 0,1\ ;\ 0,0\ ;) \\
& +(\ 0,(1-|\beta|/2)^{N_x-2}\ ;\ 0,(1-|\beta|/2)^{N_x-3}\ ;\ \cdots\ ;\ 0,1\ ;\ 0,0\ ;) \\
& \quad \ldots \\
& -(\ 0,(1-|\beta|/2)^{N_x-2}\ ;\ 0,(1-|\beta|/2)^{N_x-3}\ ;\ \cdots\ ;\ 0,1\ ;\ 0,0\ )\ \Big)
\end{aligned} \tag{5}$$

Since alternating signs are required for the different rows in the y-direction, these vectors can only be constructed when N_y is even. For $\beta > 0$, a similar pair of orthogonal vectors can be obtained by putting alternating signs in the x-direction instead; in that case there is no restriction on the value of N_y. We notice that the two zero modes defined as $\tilde{\gamma}_{L,R} = \mathbf{v}_{L,R}^T \mathbf{c}$ are not normalized yet: $\tilde{\gamma}_{L,R}^2 \neq 1$. For normalized Majorana zero modes $\gamma_{L,R} \equiv \tilde{\gamma}_{L,R}/\sqrt{C}$ to exist, the following normalization factor must be finite:

$$C = C(N_x, N_y) = N_y \sum_{i=0}^{N_x-2} (1-|\beta|/2)^{2i} = N_y \frac{1-(1-|\beta|/2)^{2(N_x-1)}}{1-(1-|\beta|/2)^2} \tag{6}$$

Clearly, $C \to \infty$ as the system size in the y-direction becomes very large. We must therefore assume N_y to be fixed and finite. In the limit $N_x \to \infty$, the normalization factor remains finite if and only if $0 < |\beta| < 4$, in which case it reads

$$\lim_{\substack{N_x \to \infty \\ N_y \text{ fixed}}} C(N_x, N_y) = N_y \frac{1}{1-(1-|\beta|/2)^2} < \infty \tag{7}$$

The existence of the two Majorana zero modes $\gamma_{L,R}$ is thus conditioned on $|\beta|$ being nonzero and smaller than the critical value $|\beta| = 4$. If this condition is satisfied, the latter are found to be exponentially localized on the left and right edges of the cylinder, respectively, as dictated by the form (4), (5) of the corresponding vectors $\mathbf{v}_{L,R}$. While uniformly spread along the y-direction, they are localized along the x-direction on a characteristic length scale $\xi = \xi(\beta) \sim 1/|\log|1-|\beta|/2||$. Remarkably, ξ is symmetric about the value $\beta = 2$, where it vanishes, and diverges as $|\beta| \to 0, 4$.

So far, we have focused on the dissipative dynamics of the bulk, generated by the cross Lindblad operators associated with the sites $i \in \mathcal{B}$. We now introduce boundary Lindblad operators L_i associated with the sites $i \in \mathcal{L}, \mathcal{R}$ belonging to the edges of the cylinder. For simplicity, we assume that the action of these additional operators is strictly local, namely, $L_i = \mathbf{l}_i^T \mathbf{c}$ with $(\mathbf{l}_i)_{2i-1} = \alpha_{2i-1}$, $(\mathbf{l}_i)_{2i} = \alpha_{2i}$, and all other components equal to zero. We then obtain

$$\text{for } i \in \mathcal{L}: \quad \begin{cases} \mathbf{l}_i^T \mathbf{v}_L &= 0 \\ \mathbf{l}_i^T \mathbf{v}_R &= \alpha_{2i}(1-|\beta|/2)^{N_x-2} \end{cases} \tag{8}$$

$$\text{and for } i \in \mathcal{R}: \quad \begin{cases} \mathbf{l}_i^T \mathbf{v}_L &= \alpha_{2i-1}(1-|\beta|/2)^{N_x-2} \\ \mathbf{l}_i^T \mathbf{v}_R &= 0 \end{cases} \tag{9}$$

As a result, when $|\beta| = 2$, the Majorana zero modes $\gamma_{L,R}$ found previously are completely unaffected by the dissipative dynamics of the edges. If this condition is not satisfied, γ_L (γ_R) is affected if and only if at least one of the coefficients α_{2i-1} (α_{2i}) does not vanish. In most cases, $\gamma_{L,R}$ thus correspond to Majorana quasi-zero modes of the full dissipative dynamics, associated with small damping rates $\lambda_{L,R}$ given by

$$\lambda_L = 2(1-|\beta|/2)^{2(N_x-2)} \sum_{i\in\mathcal{R}} |\alpha_{2i-1}|^2 \tag{10}$$

$$\lambda_R = 2(1-|\beta|/2)^{2(N_x-2)} \sum_{i\in\mathcal{L}} |\alpha_{2i}|^2 \tag{11}$$

Crucially, these rates decrease exponentially with the distance N_x between the two edges of the system, i.e. with the separation of the two localized Majorana modes.